

Calibration of the two microphone transfer function method by determining the hard wall impedance at shifted reference sections.

R. Boonen¹, P. Sas¹, W. Desmet¹, W. Lauriks², G. Vermeir²

¹ K.U.Leuven, Department of Mechanical Engineering, P.M.A.,
Celestijnenlaan 300 B, B-3001, Heverlee, Belgium

² K.U.Leuven, Laboratory for Acoustics and Thermal Physics,
Celestijnenlaan 200D, B-3001 Leuven, Belgium

e-mail: rene.boonen@mech.kuleuven.be

Abstract

In many acoustic simulations, particularly when using lumped parameter models or electrical analog circuits, the acoustic impedance of a component needs to be determined accurately. A widely used acoustic impedance measurement method is the "two microphone transfer function method", which is standardized in ISO-10534-2. When the acoustic impedance is needed over a wide frequency band with a high impedance magnitude range, this method faces some limitations. In this paper, a calibration method is proposed which uses hard wall impedance measurements at different positions of the reference section. The measured hard wall impedance is used to calibrate the microphone positions, to compensate the microphone mismatch and to estimate the wave guide damping. Also, the measured hard wall impedance can be used as performance criterion. It can be used to select frequency bands from different load impedance measurements where the accuracy is maximum and to assemble them in a load impedance measurement. As result, impedances with a high ratio with respect to the characteristic duct impedance can be accurately measured. The capability of the presented calibration method is illustrated by the impedance measurement of an open duct end and a closed tube.

1 Introduction

The measurement of acoustic impedance of materials and components is an important topic. The new directives about noise of machinery, traffic and buildings demands that preventive measures against noise have to be included in the construction design. Therefore, prior knowledge of acoustic properties of materials and components which is sufficiently accurate and reliable to use it in the design and simulation phase of new constructions is necessary. Therefore, accurate acoustic impedance measurement methods are mandatory.

The most common technique is to determine the impedance from wave reflection. The sound waves are radiated towards the sample, whereupon the waves are reflected. From the measurement of the incident and reflected waves, the reflection coefficient and the corresponding acoustic impedance are determined. The target impedance can be measured at a position different from the sensor positions. The method is suitable for the high frequency range, where wave behaviour is fully developed.

The two standardized wave reflection methods are the standing wave ratio method and the two microphone transfer function method.

This standing wave ratio (SWR, the classical Kundt duct) method determines the acoustic impedance from pressure measurements of the standing wave pattern in a duct. The method is described in the ISO-10534-1 standard [1]. The ends of the Kundt duct are closed by an excitation source at one side and the unknown

impedance at the other side. The source generates a sinusoidal signal which results in a standing wave pattern in the duct. A microphone is moved along the axis of the duct. The minimum and maximum pressure amplitude of the standing wave and the location where the minimum and maximum amplitude occur are determined. From these data, the reflection coefficient and the acoustic impedance are calculated.

The "two microphone transfer function method", which is described in ISO-10534-2 [1], has outcasted the SWR-method. The two microphone transfer function method has several advantages compared to the SWR-method. The mechanical construction of the measurement setup is simpler. The frequency band is broadened towards low frequencies. The measurements can be carried out below the first wave guide resonance up to until cross-section resonance occurs.

This method uses the transfer functions measured between two pressure sensors at two distinct positions in the measurement wave guide to determine the acoustic impedance attached at one side of the wave guide. The method is discussed in more detail in the next section.

When the acoustic impedance is needed over a wide magnitude range over a wide frequency band, the standardized impedance measurement methods face limitations. Several error mechanisms has been investigated [2, 3, 4]. Boden and Abom [2] treat the bias and random errors which occur when the transfer function between the microphones has been estimated. The conclusion was that the duct length should be kept small, the source end should be non-reflective and the first microphone should be as close as possible to the sample. The effect of the spacing between the microphones was also investigated. The maximum spacing determines the frequencies where singularities occur, i.e. where a half wave length stands between the microphone positions. Also, large errors occur when pressure nodes are present at the microphone locations. The minimum spacing is determined by the phase error sensitivity which occur when the wave-number-microphone-distance-product tends to zero.

Katz [3] presents a method to find the microphone positions with improved accuracy. The wave guide will be closed by a rigid steel plate wherein a supplementary microphone is positioned. From the tranfer function between a measurement microphone and the closed end microphone, its distance to the closed end can be estimated with higher precision than the standard ISO-method using the ruler. This action reduces the phase error sensitivity of the measurement setup.

Gibiat and Laloë [5] presents a TMTC method for the measurement of the acoustical impedance of musical instruments. The experimental setup consists of a measurement head made of brass with 15mm bore diameter and 7 mm wall thickness. To calibrate the setup, three devices with known impedance are subsequently connected. The first one is a hard wall closure at the reference section, the other two are two cavities. At each calibration impedance, the microphone transfer function will be measured. The impedance to be measured will then be expressed in terms of the three calibration impedances and the four measured transfer functions.

There lacks a performance criterion for a calibration method and measurement setup, on which the expected performance can be checked when an arbitrary unknown load impedance is connected to the measurent setup. As the performance of the impedance measurement varies widely in terms of frequency, such a criterion can be used to select the frequency bands from different measurements where they have maximum accuracy. In this way, the frequency band and the impedance magnitude range can be extended.

In this paper, a calibration method is proposed which is based on hard wall impedance measurements at different positions of the reference section. The shift of the reference section is realised by connecting closed duct ends with the same cross section as the measurement duct to the measurement duct end. The length of the duct ends represent the reference section shift. The distances between the microphones and the respective reference sections will be expressed as travelling times. As a result, the speed of sound is eliminated from the calibration procedure. The wave travelling time from each microphone position to the respective hard wall terminations will be determined by measuring the frequency at which a quarter wave length stands between the respective microphone positions and the reference section. In this way, manufacturing errors in the length of the calibration duct ends and the deviation of the position of the acoustic centre of the microphones are eliminated. The measured tranfer functions between the microphones of the calibration duct ends are used

to eliminate the sensor mismatch and to estimate the measurement wave guide damping. Then, the transfer function between the microphones is measured with the unknown impedance at the duct end. The unknown impedance will be determined in terms of the calibration transfer functions, the corresponding travelling times and the wave guide damping.

The magnitude of the measured hard wall impedance is used as a performance criterion of the setup and the calibration. A low value will indicate that the reability of the measured unknown impedance will be low. The hard wall impedance can also be used as a selection criterion between measurements at different reference sections. In this way, frequency bands wherein pressure nodes occur at the microphone position, which cause a drop in the impedance magnitude, will be replaced by parts of other measurements with correct impedance data. The outcome is an impedance measurement method which is capable to cover two decades in frequency (10 Hz-1 kHz) with a high measurement range (50 to 100× the characteristic wave guide impedance) in magnitude.

2 The two microphone transfer function method.

This section discusses the principle of the two microphone transfer function method including wave guide damping. Figure 1 presents the setup for acoustic impedance measurement. The setup consists of a straight duct which is the measurement acoustic wave guide. At the left end, an excitation source, such as a loudspeaker, is connected. At the right end, the impedance to be measured is connected. This impedance includes everything present at the right side of the reference section. Two microphones at two distinct positions x_1 and x_2 measure the sound pressure inside the duct. From the transfer function between the two microphones, the reflection coefficient and consequently, the unknown connected impedance will be determined.

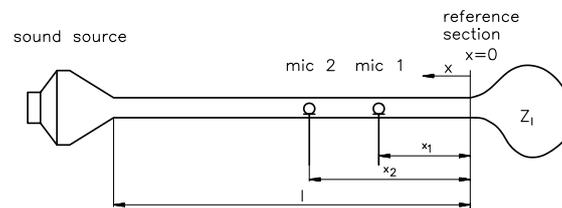


Figure 1: Wave guide with an unknown acoustic impedance Z_l .

Wave attenuation is caused by three different mechanisms. These are wall friction, heat exchange and internal gas viscosity [6]. The wave guide dimensions determine the dominant attenuation mechanism. In the frequency domain, the wave guide damping can be approximated by introducing a constant loss factor ξ in the compressibility κ of the medium [7]:

$$\kappa \approx \kappa_0 (1 + j 2 \xi) \quad (1)$$

wherein $j = \sqrt{-1}$ and κ_0 is the lossless compressibility of the medium. This type of loss factor is frequency independent and does not cause dispersion. This damping mechanism provides a good fit with the measured transfer functions in a wide frequency range, as will be demonstrated in figure 7. The effect of the loss factor ξ on the characteristic impedance Z_0 of the wave guide and the propagation constant γ is:

$$Z_0 \approx \sqrt{\frac{\rho_0 \kappa_0}{S^2}} (1 + j \xi) \quad \text{and} \quad \gamma \approx \omega \sqrt{\frac{\rho_0}{\kappa_0}} (1 - j \xi) \quad (2)$$

wherein ω is the angle frequency, ρ_0 is the density of the medium and S is the cross-section of the wave guide.

The wave pattern in the wave guide is governed by the one-dimensional Helmholtz wave equation, which describes the pressure distribution along the wave guide. At each position x , the pressure in terms of the propagation constant γ in the wave guide equals [8]:

$$p(x, \gamma) = \phi_g \frac{Z_0 Z_g}{Z_0 + Z_g} \frac{e^{-j\gamma l}}{1 - \Gamma_l \Gamma_g e^{-j2\gamma l}} (e^{j\gamma x} + \Gamma_l e^{-j\gamma x}) \quad (3)$$

wherein ϕ_g is the source volume velocity, Z_g the source internal impedance, l the distance between the exciting sound source and the reference section, Γ_l and Γ_g the reflection coefficients at the load side and source side respectively.

To measure the load impedance using the two microphone method, the transfer function T_{12} between the pressures at two distinct positions x_1 and x_2 is taken:

$$T_{12} = \frac{p(x_1, \gamma)}{p(x_2, \gamma)} = \frac{e^{j\gamma x_1} + \Gamma_l e^{-j\gamma x_1}}{e^{j\gamma x_2} + \Gamma_l e^{-j\gamma x_2}} \quad (4)$$

Notice that the source reflection coefficient drops out, the reflection coefficient at the load is the single unknown. Consequently, the choice of the source type is free. The load reflection coefficient Γ_l will then be isolated from equation (4) and the load impedance Z_l results from:

$$Z_l = Z_0 \frac{1 + \Gamma_l}{1 - \Gamma_l} = j Z_0 \frac{\sin \gamma x_1 - T_{12} \sin \gamma x_2}{\cos \gamma x_1 - T_{12} \cos \gamma x_2} \quad (5)$$

3 Improved calibration method

Ideally, the impedance of a hard wall at the reference section is infinite. In the laboratory, the hard wall impedance will always be finite due to the measurement imperfections. The magnitude of the measured impedance can be used as a quality criterion for the setup and the calibration procedure. The design of the setup and the calibration procedure should result in a closed end impedance as high as possible. After calibration, the unknown impedance can be connected to the reference section. The range in which the unknown impedance can be measured depends on the magnitude of the measured hard wall impedance.



Figure 2: Laboratory setup for acoustic impedance measurement.

The laboratory setup, used to investigate the calibration method, is presented in figure 2. It consists of a thick-walled steel duct with 40 mm internal diameter and 1.5 m length. At the back end sits a 60 W horn driver. Two PCB-106B pressure sensors are positioned at a distance $x_1 = 0.3$ m and $x_2 = 0.47$ m from the reference section. A HP-3562 signal analyser excites the horn driver with a stepped sine signal and measures the transfer function between the two sensors, from which the acoustic impedance connected to the reference section will be determined.

To calibrate the setup, the transfer function will be measured with the waveguide closed at the reference section. Thereafter, the reference section will be shifted to another position by interconnecting a short waveguide. A new transfer function will be measured. This procedure can be repeated several times with different lengths of interconnected waveguides. From the obtained transfer functions, the waveguide can be calibrated. The criterion is the maximization of the hard wall impedance. At least two transfer functions are necessary to calibrate the setup.

In this investigation, three transfer functions are used. The first one, T_{12} , is measured with the reference section at $x_1 = 0.3$ m and $x_2 = 0.47$ m, as presented in figure 3. The second one, T_{34} , is measured with the reference section shifted 47 mm, so $x_3 = 0.347$ m and $x_4 = 0.517$ m, as presented in figure 4. The third one, T_{56} , is measured with the reference section shifted 302 mm, so $x_5 = 0.602$ m and $x_6 = 0.779$ m.

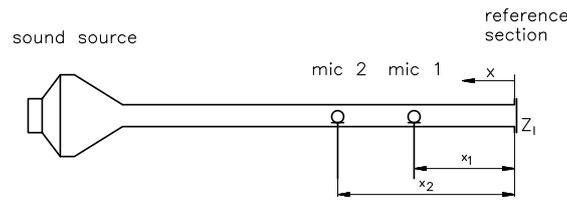


Figure 3: Calibration setup with duct end closed at the reference section.

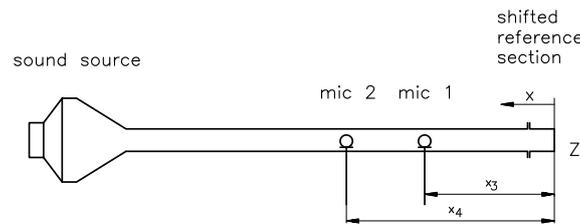


Figure 4: Calibration setup with duct end closed at the shifted reference section.

The following steps in the calibration procedure will be performed.

- The distances between the microphones and the reference section are expressed in terms of travelling times. In this way, the speed of sound is eliminated from the calibration process.
- The sensor mismatch will be eliminated.
- The wave guide damping will be estimated.
- The singularities occurring in the frequency band of interest can be removed using additional transfer functions at other reference sections.

3.1 Elimination of the speed of sound

The aim of the elimination of the speed of sound from the calibration procedure is to avoid the measurement of the distance between the acoustic centers of the microphones, the ambient pressure and the temperature. In this way, deviations in these measured values are eliminated from the calibration procedure.

The distances x_1 and x_2 in expression (5) can be substituted by the travelling times t_1 and t_2 needed for the wave to travel from these positions to their reference sections respectively. The relation between the travelling times and their respective distances is:

$$t_1 = \frac{x_1}{v_{ph}} \quad \text{and} \quad t_2 = \frac{x_2}{v_{ph}} \quad (6)$$

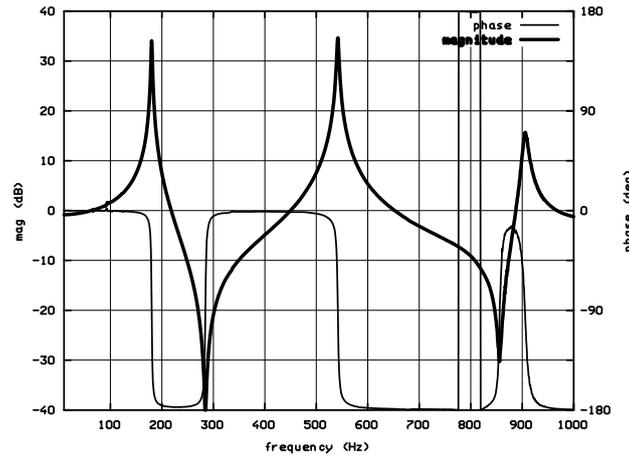


Figure 5: Measured transfer function T_{12} between the sensors located at $x_1 = 0.3$ m and $x_2 = 0.47$ m with the duct closed at the reference section.

wherein $v_{ph} = \frac{\omega}{\text{Re}(\gamma)}$ is the phase velocity of the sound. The resulting transfer function T_{12} in terms of travelling times will be:

$$T_{12} = \frac{\delta (Z_c \cos \beta t_1 + j Z_0 \sin \beta t_1)}{(Z_c \cos \beta t_2 + j Z_0 \sin \beta t_2)} \quad (7)$$

wherein Z_c is the measured impedance of the closed waveguide, $\beta = \omega (1 - j \xi)$ and δ the microphone mismatch.

The travelling times t_1 and t_2 are estimated from the measured transfer function T_{12} , as presented in figure 5. They correspond to the first pole for the farthest microphone and the first zero for the nearest microphone position. The pole and the zero correspond to the first node of the pressure distribution of the standing wave appearing at the positions x_1 and x_2 respectively. The travelling times t_1 and t_2 equal:

$$t_1 = \frac{1}{4 f_1} \quad \text{and} \quad t_2 = \frac{1}{4 f_2} \quad (8)$$

in which the frequencies f_1 and f_2 are associated to the frequencies determined by the quarter wavelength between the reference section and the positions x_1 and x_2 respectively.

This procedure is applied to all the measured transfer functions. For the transfer function T_{34} , where x_3 takes the place of x_1 and x_4 the place of x_2 , the travelling times will be:

$$t_3 = \frac{1}{4 f_3} \quad \text{and} \quad t_4 = \frac{1}{4 f_4} \quad (9)$$

wherein the frequencies f_3 and f_4 correspond to the quarter wave lengths between the positions x_3 and x_4 and the reference section respectively.

Similar for the transfer function T_{56} , where x_5 takes the place of x_1 and x_6 the place of x_2 , the travelling times will be:

$$t_5 = \frac{1}{4 f_5} \quad \text{and} \quad t_6 = \frac{1}{4 f_6} \quad (10)$$

wherein the frequencies f_5 and f_6 correspond to the quarter wave lengths between the positions x_5 and x_6 and the reference section respectively.

3.2 Elimination of the microphone mismatch

The electrical transfer functions between pressure and voltage of the microphones have to be eliminated. By considering the ratio T_{c1} between the two measured transfer functions T_{12} and T_{34} , the sensor mismatch δ vanishes from numerator and denominator:

$$T_{c1} = \frac{T_{12}}{T_{34}} = \frac{\delta (Z_{c1} \cos \beta t_1 + j Z_0 \sin \beta t_1)}{(Z_{c1} \cos \beta t_2 + j Z_0 \sin \beta t_2)} \cdot \frac{(Z_{c1} \cos \beta t_4 + j Z_0 \sin \beta t_4)}{\delta (Z_{c1} \cos \beta t_3 + j Z_0 \sin \beta t_3)} \quad (11)$$

$$T_{c1} = \frac{z_{c1}^2 \cos \beta t_1 \cos \beta t_4 - \sin \beta t_1 \sin \beta t_4 + j z_{c1} \sin \beta t_1 \cos \beta t_4 + j z_{c1} \cos \beta t_1 \sin \beta t_4}{z_{c1}^2 \cos \beta t_2 \cos \beta t_3 - \sin \beta t_2 \sin \beta t_3 + j z_{c1} \sin \beta t_2 \cos \beta t_3 + j z_{c1} \cos \beta t_2 \sin \beta t_3} \quad (12)$$

wherein $z_{c1} = Z_{c1}/Z_0$ is the normalized closed end impedance, which is the ratio between the closed end impedance Z_{c1} and the characteristic measurement wave guide impedance Z_0 . z_{c1} will result from the measurement of the transfer functions T_{12} and T_{34} and will have a finite value caused by the measurement imperfections.

The effect of the finite sensing surface of the microphones has been investigated analytically by integrating the pressure distribution of the standing waves inside the duct over the microphone surface. An effect was observed on the individual transfer functions T_{12} and T_{34} , but it vanishes in the transfer function ratio together with the microphone mismatch.

Figure 6 presents the ratio T_{c1} between the measured transfer functions T_{12} and T_{34} .

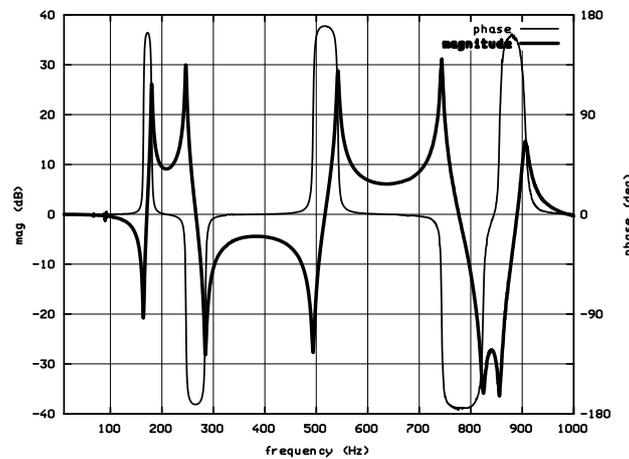


Figure 6: Ratio between the two transfer functions $T_{c1} = T_{12}/T_{34}$

In the same way, the ratio T_{c2} between the transfer function T_{12} and T_{56} is determined. The expression of T_{c2} is similar to the one of T_{c1} , except that t_3 is substituted by t_5 and t_4 by t_6 . From this expression, the normalized closed end impedance $z_{c2} = Z_{c2}/Z_0$ will result in stead of z_{c1} .

3.3 Determination of the wave guide damping

If the wave guide is ideally closed, the transfer function given in equation (12) simplifies to:

$$T_{c0} = \frac{\cos \beta t_1 \cos \beta t_4}{\cos \beta t_2 \cos \beta t_3} \quad (13)$$

The ratio between the transfer function T_{c0} and the measured transfer function T_{c1} is almost unity, except at the poles and the zeros. Apart from the poles and the zeros, the loss factor ξ is the only unknown and will be determined numerically from $T_{c1} - T_{c0} = 0$.

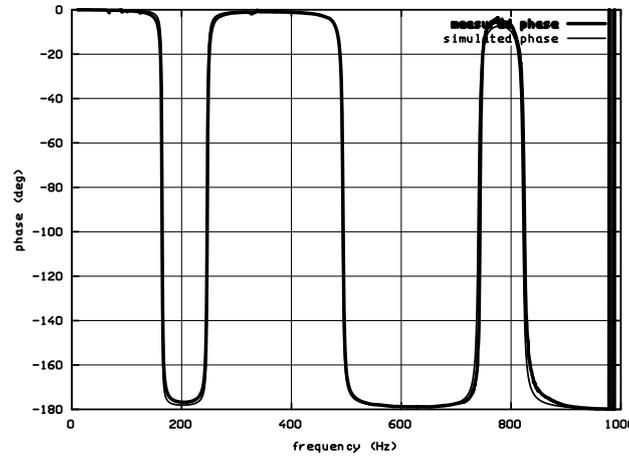


Figure 7: Comparison between the phase of the measured transfer function T_{12} (thick line) and the phase simulated using expression (7) (thin line).

The obtained loss factor ξ can be introduced as a hysteretic damping for the measured frequency domain. Figure 7 displays the overlay of the phase of the measured transfer function T_{12} (thick line) and the phase of equation (7) (thin line). The damping ξ , estimated by the previously described method, is introduced in $\beta = \omega (1 - j \xi)$. The deviation between the two phases remains very small.

3.4 Determination of the closed end impedance

After introducing the loss factor ξ in the transfer functions T_{c1} expressed by equation (12), the normalized acoustic impedance z_{c1} of the closed end can be determined from the measured transfer function presented in figure 6. The resulting normalized closed end impedance z_{c1} is presented in figure 8 in thick line. This normalized impedance defines the magnitude measurement range. It must be as high as possible. The expression (12) is quadratic in z_{c1} , resulting in two solutions. One solution corresponds to the direct reference section, the other to the shifted reference section. The solution corresponding to the highest impedance is selected at each frequency point. In the same way, the normalized closed end impedance z_{c2} is determined from T_{c2} and displayed in figure 8 in thin line. At each frequency, the maximum value of the two resulting closed end impedances will be selected, resulting in the selection function displayed at the bottom of figure 8. When the selection function is low, the value in thick line is selected, otherwise the value in thin line is selected. The resulting normalized closed end impedance z_c will be the envelope of the impedances z_{c1} and z_{c2} . This selection function will be used to determine the unknown impedance, to overlap the singularities. The measurement range, given by the closed end impedance z_c , reaches 40 dB ($Z_c \approx 100 \times Z_0$) between 100 Hz and 400 Hz, and 30 dB ($Z_c \approx 30 \times Z_0$) in the rest of the frequency band. The measurement range can be further extend by adding additional transfer functions at other reference section positions.

4 Determination of the unknown impedance

After calibration, the unknown impedance will be determined. For that purpose, the unknown impedance is connected to the wave guide at the reference section and the transfer function T_l between the microphones is measured. The unknown impedance Z_l will be calculated with respect to each closed end impedance z_{c1} and z_{c2} obtained in the previous section.

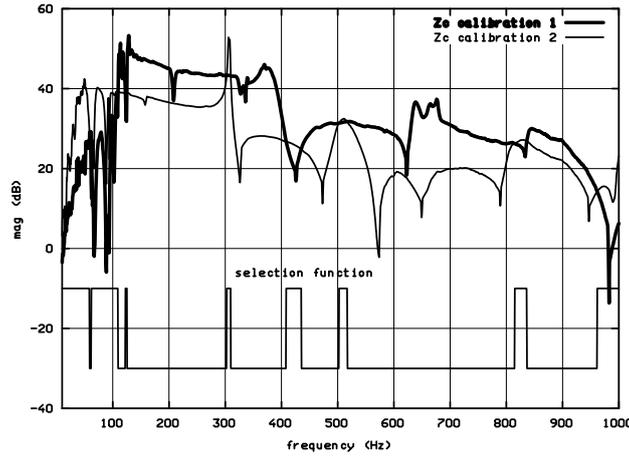


Figure 8: Resulting closed end impedance amplitude Z_c (dB(ref Z_0)) applying expression (12) to the measured transfer function T_c .

To remove the sensor mismatch δ , the transfer function ratio T_{l1} is derived in a similar way as equation (12):

$$T_{l1} = \frac{T_l}{T_{34}} = \frac{\delta (Z_{l1} \cos \beta t_1 + j Z_0 \sin \beta t_1)}{(Z_{l1} \cos \beta t_2 + j Z_0 \sin \beta t_2) \frac{(Z_{c1} \cos \beta t_4 + j Z_0 \sin \beta t_4)}{\delta (Z_{c1} \cos \beta t_3 + j Z_0 \sin \beta t_3)}} \quad (14)$$

wherein Z_{l1} is the unknown impedance corresponding to x_3 and x_4 as distances between the microphones and the reference section. The normalized unknown impedance $z_{l1} = Z_{l1}/Z_0$ will result in:

$$z_{l1} = \frac{(\sin \beta t_1 \sin \beta t_4 - T_{l1} \sin \beta t_2 \sin \beta t_3) + j z_{c1} (T_{l1} \sin \beta t_2 \cos \beta t_3 - \sin \beta t_1 \cos \beta t_4)}{z_{c1} (T_{l1} \cos \beta t_2 \cos \beta t_3 - \cos \beta t_1 \cos \beta t_4) + j (\cos \beta t_1 \sin \beta t_4 - T_{l1} \cos \beta t_2 \sin \beta t_3)} \quad (15)$$

wherein $T_{l1} = T_l/T_{34}$.

Similarly, the normalized unknown impedance $z_{l2} = Z_{l2}/Z_0$ will result in:

$$z_{l2} = \frac{(\sin \beta t_1 \sin \beta t_6 - T_{l2} \sin \beta t_2 \sin \beta t_5) + j z_{c2} (T_{l2} \sin \beta t_2 \cos \beta t_5 - \sin \beta t_1 \cos \beta t_6)}{z_{c2} (T_{l2} \cos \beta t_2 \cos \beta t_5 - \cos \beta t_1 \cos \beta t_6) + j (\cos \beta t_1 \sin \beta t_6 - T_{l2} \cos \beta t_2 \sin \beta t_5)} \quad (16)$$

wherein $T_{l2} = T_l/T_{56}$ and z_{l2} is the normalized unknown impedance corresponding to x_5 and x_6 as distances between the microphones and the reference section. The resulting normalized unknown impedance z_l will be assembled by selecting the proper z_{l1} and z_{l2} using the same selection criterion to form the envelope of the normalized closed end impedance z_c . In this way, the singularities will overlap and the measurement range will be extended.

5 Test cases

To demonstrate the capabilities of the presented acoustic impedance calibration method, the open duct end and a closed tube are presented as test cases.

As first test case, the open duct impedance has been measured. The open duct impedance is the other extreme of the closed duct impedance and analytical expressions are available to validate the result [9].

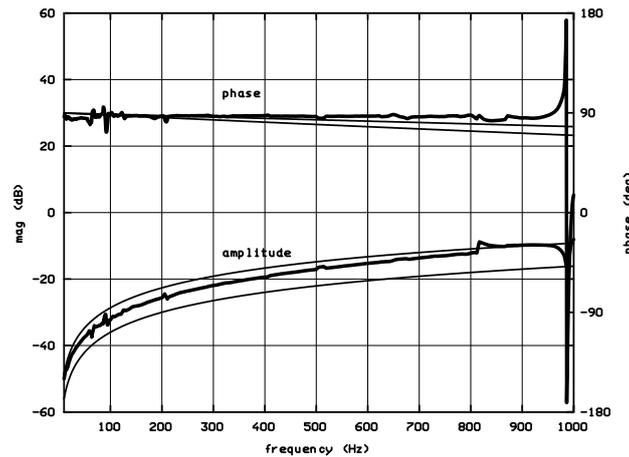


Figure 9: Resulting open end impedance (thick line) after improved calibration compared to the analytical expressions for the spherical radiator impedance and the piston in infinite baffle (thin lines). (dB(ref Z_0))

In figure 9, the thick line presents the resulting measured open end impedance in magnitude and phase, normalised to the characteristic wave guide impedance Z_0 . The duct end is flanged at the reference section with a flange of 120 mm diameter. The solution situates between the spherical radiator and the infinite baffle, for which analytical solutions are available. The lower thin line in the amplitude combined with the upper thin line in the phase represents the impedance calculated from the analytical expression of the spherical wave radiator. The other combination of thin lines represent the impedance calculated from the analytical expression of a piston in an infinite baffle. The amplitude of the measured open end impedance situates between these two extreme cases. The measured phase situates slightly above the phase of the two cases.

The second test case is a tube with 40 mm diameter and 300 mm length, terminated by a hard wall. Figure 10

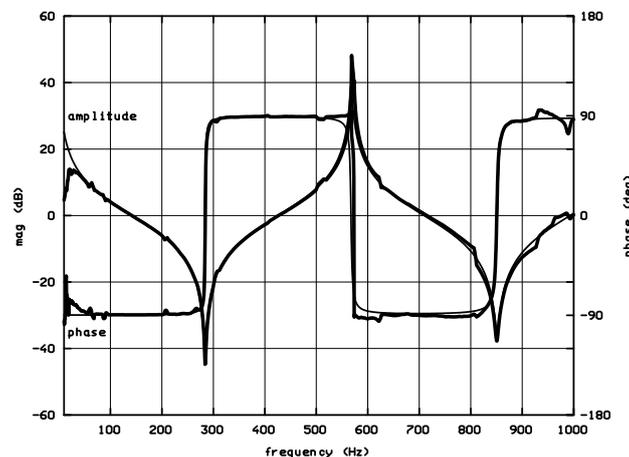


Figure 10: Measured acoustic impedance (thick line) of a piece of duct of 300 mm length compared to the analytical solution (thin line). (dB(ref Z_0))

presents the measured acoustic impedance in thick line in amplitude and phase, normalized to the characteristic wave guide impedance Z_0 . The analytical expression of the normalized impedance z of a closed tube is given by:

$$z = -j \cot \gamma l \quad (17)$$

wherein γ is the propagation constant and l the length of the tube. This normalized impedance is also plotted in figure 10 in amplitude and phase in thin line. Both plots are consistent. Below 30 Hz, the acoustic

impedance measurement is limited by the low response of the pressure sensors at low frequency. This effect is also observed in figure 8. The switching of the selection of z_l can be observed around 500 Hz, 800 Hz and 900 Hz. The distance of 80 dB between the top and the bottom values of the measured impedance gives an indication of the magnitude of the measurement range using the presented calibration method.

6 Conclusion

The presented calibration method improves the measurement accuracy of acoustical impedance. It is based on measurements of the hard wall impedance at different positions of the reference section. The deviations caused by measuring the distances between the acoustic centers of the microphones and the reference section, the ambient pressure and the temperature are eliminated by the substitution of the wave travelling distances between the respective microphone positions and the reference section by the corresponding wave travelling times. The sensor mismatch vanishes when the ratios between the transfer functions between the microphones at several reference positions are determined. The final hard wall impedance is composed by selecting the maximum of the measured hard wall impedances resulting from each transfer function ratio at each reference section position at each frequency. The same selection mechanism is used to compose the impedance of the unknown impedance. The outcome is an impedance measurement method with a high impedance range in magnitude, ranging from 30 to 40 dB around the characteristic impedance of the measurement wave guide.

Acknowledgments.

The author thanks the FWO (Fonds Wetenschappelijk Onderzoek) for funding the research project.

References

- [1] ISO 10534, *Determination of sound absorption coefficient and impedance in impedance tubes*, International Organisation for Standardization, Case postale 56, CH-1211 Genève 20, (1998).
- [2] H. Bodén and M. Åbom, *Influence of errors on the two microphone method for measuring acoustic properties in ducts*. Journal of Acoust. Soc. Am., Vol. 79, No. 2, (1986), pp. 541-549.
- [3] B.F.G. Katz, *Method to resolve microphone and sample location errors in the two-microphone duct measurement method*. Journal of Acoust. Soc. Am., Vol. 108, No. 5, (2000), pp. 2231-2237.
- [4] Paul Dickens, John Smith and Joe Wolfe, *Improved precision in measurements of acoustic impedance spectra using resonance-free calibration loads and controlled error distribution*, Journal of Acoust. Soc. Am., Vol. 121, No. 3, (2007), pp. 1471-1481.
- [5] V. Gibiat and F. Laloë, *Acoustical impedance measurements by the two-microphone-three-calibration (TMT) method*, Journal of Acoust. Soc. Am., Vol. 88, No. 6, (1990), pp. 2533-2545.
- [6] A. D. Pierce, *Acoustics: An introduction to its physical principles and applications*, Mc-Graw-Hill, (1981)
- [7] E.J. Scudrzyk, *Foundations of Acoustics*, Springer Verlag (1972)
- [8] H. P. Neff, Jr, *Basic Electromagnetic Fields*, Harper & Row, (1987)
- [9] L. L. Beranek, *Acoustics*, Mc Graw-Hill, (1954)

- [10] R. Boonen, P. Sas, *Calibration of the two microphone transfer function method to measure acoustic impedance in a wide frequency range*. Proceedings of The ISMA2004 Conference, Leuven, Belgium, Vol I, (2004), pp. 325-336.
- [11] R. Boonen, P. Sas, *Determination of the acoustic impedance of an internal combustion engine exhaust*. Proceedings of The ISMA2002 Conference, Leuven, Belgium, Vol V, (2002), pp. 1939-1946.